

Manipulating ionization path in a Stark map: Stringent schemes for the selective field ionization in highly excited Rb Rydberg atoms

M. Tada ^{a,*}, Y. Kishimoto ^a, M. Shibata ^a, K. Kominato ^a,
S. Yamada ^b, T. Haseyama ^a, I. Ogawa ^{a,2}, H. Funahashi ^b,
K. Yamamoto ^c, S. Matsuki ^a

^a*Nuclear Science Division, Institute for Chemical Research, Kyoto University,
Gokasho, Uji, Kyoto 611-0011, Japan*

^b*Department of Physics, Kyoto University, Kyoto 606-8503, Japan*

^c*Department of Nuclear Engineering, Kyoto University, Kyoto 606-8501, Japan*

Abstract

We have developed a quite stringent method in selectivity to ionize the low angular-momentum (ℓ) states which lie below and above the adjacent manifold in highly excited Rb Rydberg atoms. The method fully exploits the pulsed field-ionization characteristics of the manifold states in high slew-rate regime: Specifically the low ℓ state below (above) the adjacent manifold is firstly transferred to the lowest (highest) state in the manifold via the adiabatic transition at the first avoided crossing in low slew-rate regime, and then the atoms are driven to a high electric field for ionization in high slew-rate regime. These extreme states of the manifold are ionized at quite different fields due to the tunneling process, resulting in thus the stringent selectivity. Two manipulation schemes to realize this method actually are demonstrated here experimentally.

Key words: Rydberg atom, field ionization, Stark effect

PACS: 32.80.Rm, 32.60.+i, 79.70.+q

* Corresponding author.

Email address: tada@carrack.kuicr.kyoto-u.ac.jp (M. Tada).

¹ Present address: Research Center for Neutrino Science, Tohoku University, Sendai 980-8578, Japan

² Present address: Department of Physics, Osaka University, Toyonaka, Osaka 560-0043, Japan

One of the attractive characteristics of the Rydberg atoms is that they couple strongly to the external electromagnetic field[1,2]. From this property, it has been proposed that the atoms are utilized for a single photon detector in the microwave range[3,4] besides a number of other applications in fundamental physics research such as the cavity quantum electrodynamics [5]. In fact the electric dipole transition matrix elements between the states with principal quantum number n and $n \pm 1$ are larger with increasing n (proportional to $n^2 a_0$, where a_0 is the Bohr radius) and yet the lifetime of these states is long enough (proportional to n^3 for the low ℓ ($\ell \ll n$) states) to be utilized for this purpose. In actual schemes along this line, the Rydberg atoms, excited from the initially prepared lower state to a upper state by absorbing microwave photons, are selectively ionized by means of the field ionization.

In order to utilize the Rydberg atoms as a microwave single-photon detector, it is therefore essential to field-ionize the lower and the upper states selectively. In the Rydberg states with n less than 50, where the corresponding photons are in the millimeter to sub-millimeter wave region, this selectivity is mostly achieved by fully exploiting the adiabatic transitions in the time evolution of atoms in the Stark map[1,2]. However this ionization scheme has increasing difficulty to achieve good selectivity for the higher excited Rydberg states because the difference in the ionization field for these states via the adiabatic transitions is smaller with increasing n . Moreover the non-adiabatic process becomes dominant for the higher excited Rydberg states, thus the efficiency for the selection is correspondingly reduced with this conventional scheme.

In this Letter we present a new stringent method to selectively ionize the highly excited Rydberg atoms with n larger than 90; this new method is realized by choosing, as the lower and the upper states, two low angular-momentum (ℓ) states which lie below and above the adjacent manifold. The ionization paths are then manipulated for the chosen two states in the following way. Firstly the low l state below (above) the adjacent manifold is transferred to the lowest (highest) state in the manifold through the first avoided crossing with a slowly varying (low slew-rate) pulsed electric field. Then a pulsed field is applied to drive the manifold states into the ionization along the non-adiabatic paths in the Stark structure in high slew rate regime.

The stringent selectivity in the above ionization scheme now results from the characteristics of the field ionization process for the manifold states as revealed in our previous work[6]: In fact the tunneling process in the field ionization is increasingly the dominant process in the highly excited Rydberg atoms with increasing $n > 90$ [6]. The ionization field value with this process depends strongly on the energy position in the split manifold states as well known in Hydrogen atom [1,2], that is, the ionization field value is higher in the higher energy (bluer) state than in the lower energy (redder) state. The ionization field values for the lowest and the highest states of $n=120$ manifold in Rb, for

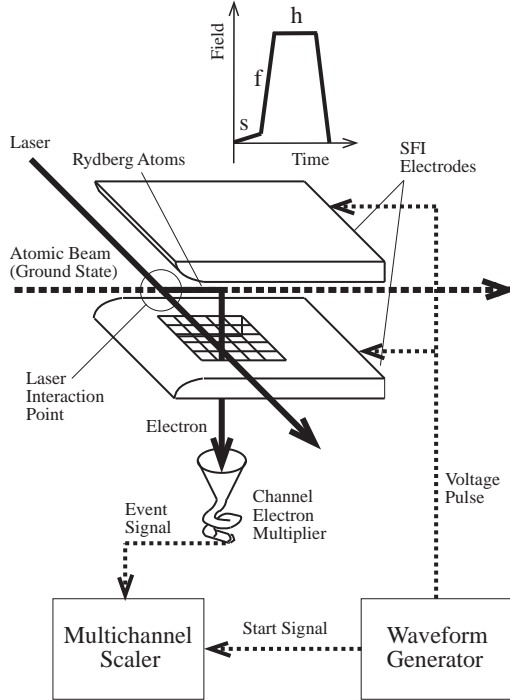


Fig. 1. Schematic diagram of the present experimental setup. An example of the applied pulse profile is shown at the top, in which s , f and h denote the components of slow, fast and holding time of the pulse, respectively.

example, are 4.5 and 10.5 V/cm, respectively, quite large difference compared to the case of the adiabatic transition scheme mentioned earlier. The effectiveness and universality of the present scheme are demonstrated here in the highly excited Rydberg states of Rb.

Schematic diagram of the present experimental setup is shown in Fig. 1. A thermal atomic beam of Rb was introduced to the center of the field ionization electrodes, where the ^{85}Rb atoms in the ground state $5s_{1/2}$ were excited to the ns and np states through the second excited $5p_{3/2}$ state by the two-step laser excitation. A diode laser (780 nm) and a dye laser (479 nm) with a dye of coumarin 102 pumped by a Kr ion laser were used for the first and second step excitations, respectively. The polarizations of the laser lights adopted in the present experiment are parallel and perpendicular to the electric field applied for the first and the second lasers, respectively³.

The electrodes consist of two parallel plates of 52 mm length and 40 mm width, the distance between them being 24 mm. A pulsed electric field was applied to the electrodes for the field ionization in the present experiment. For this purpose a sequence of voltage pulse was generated by a waveform generator

³ No appreciable change in the experimental results was observed, however, with other configurations such as both parallel and perpendicular cases.

AWG420 (Sony Tektronix) and amplified by fast amplifiers before applying to the electrodes. The pulse profile adopted here has mainly three components, slow (s), fast (f) and holding (h) parts as shown in Fig. 1; the slow component s is used for transferring the low ℓ states into the manifold states, while the fast component f is to ionize the manifold states in high slew rate regime as will be explained in detail later. The component h is used for an advanced pulse profile to improve and enhance the selectivity more. The pulse profile adopted for each measurement will be shown later together with the experimental data⁴.

The electrons liberated by the field ionization were guided to a channel electron multiplier through two fine-mesh grids placed in one of the electrode plates. Ionization signals of electrons from the channel electron multiplier were amplified by a preamplifier and a main amplifier and then fed to a multichannel scaler P7886 (FAST ComTek) after the pulse height discrimination. The ionization events were counted as a function of the elapsed time from the starting time of the ramp field with the dwell time of 500 ps. From the correspondence of the applied electric field and the time bin, the observed timing spectra were converted into the field ionization spectra as a function of the applied electric field.

As the first step for the selective field ionization, two schemes of *forward* and *backward* drivings for the manipulation of the ionization path were examined experimentally;

1) *forward driving* scheme: Typical pulse profile applied for this scheme is shown in Fig. 2 together with the Stark structure around $n = 108$ manifold for $|m_j| = 1/2$. The Stark energy structure was calculated with the matrix diagonalization method[9]. The relevant energy levels here are the $111s$ (lower) and $111p$ (upper) states which are below and above the adjacent 108 manifold, respectively, as shown in the top of the figure. In order to transfer the initially excited s and p states into the manifold states, a linearly ramped field is first applied to the atoms up to ~ 80 mV/cm. Here the slew rate of the applied field is slow enough (less than 1 mV/(cm $\cdot\mu$ s)) to cause the s (p) state transfer adiabatically to the lowest (highest) manifold state⁵. Then the atoms

⁴ Repetition rate of the applied pulse was typically 5 kHz. The rate does not give any effect on the experimental results and conclusion presented here, but is related to the detection efficiency of the Rydberg atoms since we used cw atomic beam in the present experiment. The detection efficiency depends on various experimental factors, maximum being about 80 %.

⁵ Detailed slew rate dependences of the transition probabilities for the adiabatic and non-adiabatic processes at the first avoided crossings of the s (and also the p) state and the adjacent manifold states were measured in a separate experiment and compared with theoretical predictions taking into account the multilevel-crossing effect. Detailed results of these studies will be presented elsewhere.

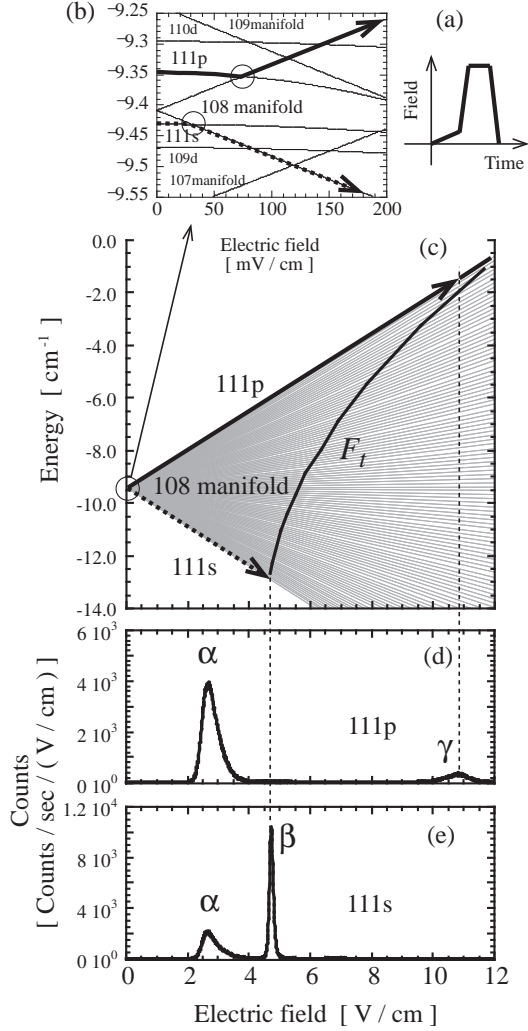


Fig. 2. Stark energy diagrams near the $n = 108$ manifold and field ionization spectra of the $111p$ and $111s$ states in the *forward driving* scheme. See the pulse profile (a) here and also the text for the meaning of the *forward driving*. (a) Schematic pulse profile applied. Here the slow component is exaggerated to see easily. (b) and (c) Stark energy diagrams near the $n=108$ manifold; (b) Enlarged Stark map at the low electric field, where only the lowest and the highest energy states in the manifold are drawn for clarity. (c) Stark energy diagram covering over the region from zero to the ionization field. Solid line (F_t) drawn in the split Stark energy levels of 108 manifold is the ionization field expected from the tunneling process. Manipulated path trajectories in the Stark energy structure for the ionization of $111p$ and $111s$ states are also shown both in (b) and (c) with thick solid and thick dotted lines, respectively. (d) and (e) Field ionization spectra of p and s states in the *forward driving* scheme; (c) $111p$ state and (d) $111s$ state.

are driven for ionization to high electric field with the same direction to the preceding slow component, here in this case up to 14 V/cm, with a slew rate of 13.4 V/(cm· μ s). The observed ionization spectra resulting from the applied pulse field are shown also in Fig. 2. As presented in detail in our previous

investigation[6], the high field peaks in the spectra (peaks γ and β in Figs. 2d and 2e, respectively) come from the tunneling process and the values of the ionization field corresponding to these peaks are quite different. We call this scheme *forward driving* scheme.

2) *backward driving* scheme: In Fig. 3a shown is the pulse profile applied for this scheme, where the initially applied slow component and the following fast pulse component of the electric field have opposite polarity. The reversed electric field causes the atoms driven to zero field once after the transition to the manifold states and then driven to higher electric field for ionization. This reversed (*backward*) driving of the applied electric field makes the ionization path completely different from the case of the *forward* driving: In fact the peaks due to the tunneling process for the p and s states in Figs. 3d and 3e have reversed positions to those shown in Figs. 2d and 2e in their ionization fields. This kind of reversed driving in the ionization process has been previously studied by Harmin[7] theoretically and also by several groups [8] experimentally but only at lower n region. More detailed characteristics of this *backward driving* scheme revealed systematically in the present experiment will be presented elsewhere.

The above two driving schemes have different features as revealed in the observed spectra: 1) The fraction of the tunneling-process component to the total ionization signals for the $111p$ state is larger in the case of *backward driving*, 2) the width of the component for the $111p$ state in the *backward driving* is narrower than in the *forward driving*. These features indicate that the *backward driving* scheme is superior for the microwave single-photon detector from the view point of the selectivity and the detection efficiency, although the peak position of the tunneling-process component for the $111p$ state is in between the two peaks for the $111s$ state.

It is also noted here that a small peak (denoted by β) observed in between the two prominent peaks (α and γ) in Fig. 3e in the ionization spectrum of $111s$ state is due to the transition induced by the blackbody radiations from the initially prepared $111s$ state to the neighboring p states: In fact this peak position corresponds exactly to that observed in the excitation of the $111p$ state as seen in Fig. 3d. The observed ratio (2%) of this peak component to that of the initially excited $111s$ component is also in rough agreement with the value (3%) estimated from the relevant transition rates under the actual experimental conditions. The origin of this peak was further confirmed by introducing a microwave source into the present experimental system, where the source frequency is tuned to the transition frequency from the $111s_{1/2}$ to the $111p_{3/2}$ states; in Fig. 3f shown is the enhanced peak due to the effect of this microwave source ⁶. Manipulating the ionization path as described

⁶ Similar transition component would be also expected in the counter case of

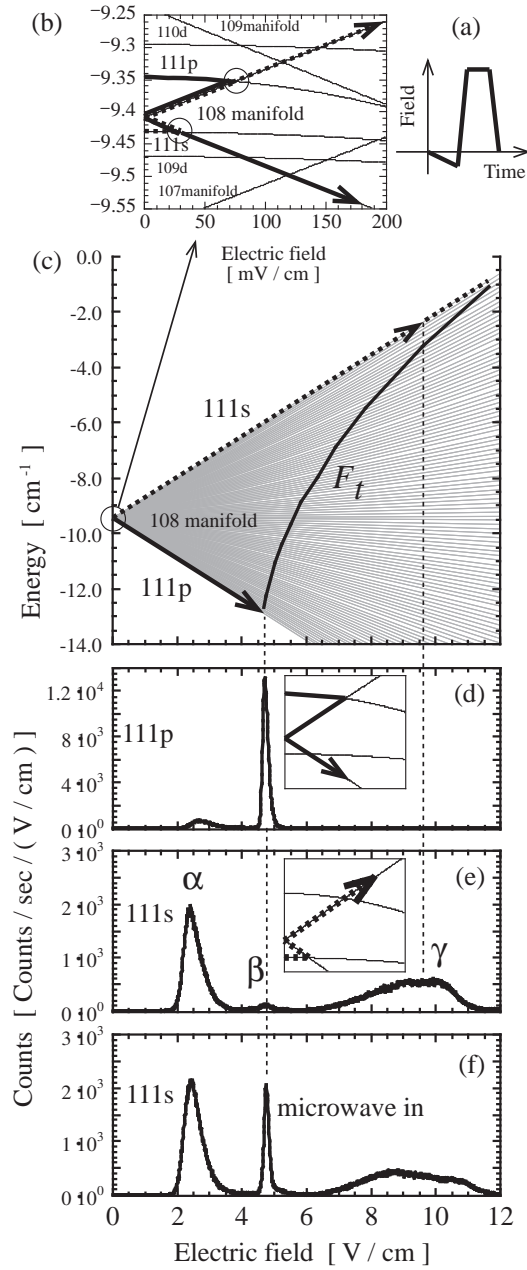


Fig. 3. Stark energy diagrams near the $n = 108$ manifold and field ionization spectra of the $111p$ and $111s$ states in the *backward driving* scheme. The applied pulse profile is shown at the top right (a). Here the slow component is exaggerated to see easily. See the pulse profile here and also the text for the meaning of the *backward driving*. (b) and (c) The same Stark energy diagrams near the $n=108$ manifold as in Fig. 2 except for the manipulated path trajectories in the ionization of $111p$ and $111s$ states. (d) - (f) Field ionization spectra of p and s states in the *backward driving* scheme. Manipulated path trajectories at the low field region in the ionization process are schematically shown in the inset of (d) and (e); (d) $111p$ state, (e) $111s$ state, (f) $111s$ state initially excited with microwave source in.

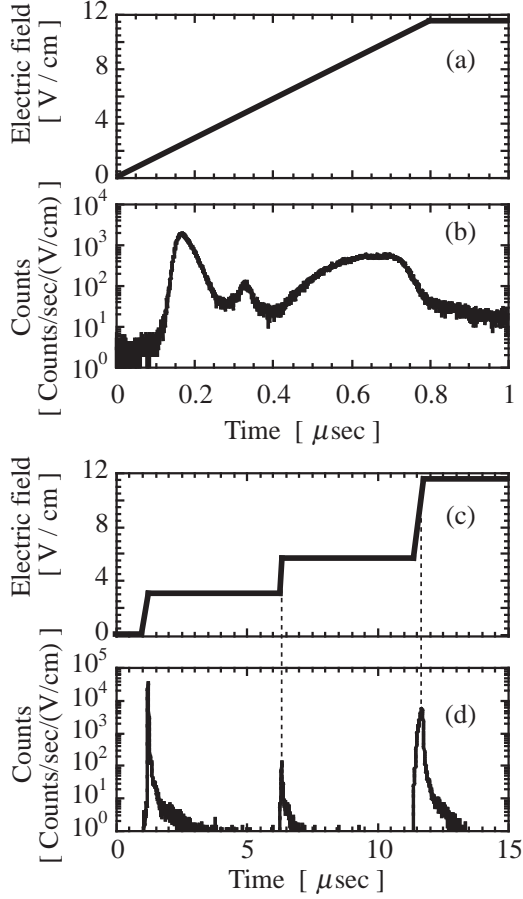


Fig. 4. Pulse profile and the corresponding field ionization spectrum of the $111s$ state obtained with the advanced *three-step* field ionization scheme together with those for the standard *one-step* scheme presented in Fig. 3. Note here that the slow component of the applied pulse in this *backward driving* scheme is omitted both in the profile drawing of (a) and (c) for simplicity. (a) and (b) *One-step* pulse profile adopted in the previous standard *backward driving* scheme as presented in Fig. 3 and corresponding timing spectrum in logarithmic scale. (c) and (d) Advanced *three-step* pulse profile in the *backward driving* scheme and corresponding timing spectrum observed.

above was thus found to be quite effective to selectively ionize the low ℓ states below and above the adjacent manifold. However the lower peak (α) due to the autoionization-like process is rather broad and has a tail component which extends to the region of the peak (β) due to the blackbody induced transitions as noted above. The extension of this tail part to the transition component is more clearly seen in Fig. 4b where a raw timing spectrum is shown in logarithmic scale.

forward driving scheme. This component is, however, too small to be seen clearly in the spectrum shown in Fig. 2e because of its small relative ratio to the lower peak from the autoionization-like process and also of its broad distribution.

In order to improve the selectivity further more, the applied pulse profile was modified as shown in Fig. 4c; essential modification here is that the pulse profile at the ionization stage is divided into three parts, in each of which the applied electric field is held for some period before proceeding to the next step of ionization. Each part of the pulse profile is used to induce the field ionization corresponding to each peak observed in the previous scheme as seen in Fig. 4b. However this division of the pulse profile into three parts is not just for dividing the ionization spectra into three in which each of the three peaks is just included. Instead this pulse profile actually enhances the separation between the low field ionization (portion α in Fig. 3e) of the autoionization-like process and the following ionization related to the $s - p$ transition (portion β in Fig. 3e) as clarified actually in Fig. 4d. This is because the ionization at the portion α has a finite lifetime, which depends strongly on the applied electric field [9], and even at the lower electric field than its peak field, the atoms relevant to this ionization process are ionized within the holding time ($5 \mu\text{s}$ in the present case) longer than their lifetimes. Since the ionization field value to be held for this part can be chosen in such a way that at this lower field the atoms in the upper p state are not ionized at all, the extended tail of the lower peak α which entered into the peak region of the portion β in the previous *one-step backward driving* scheme is almost completely removed out in this new *three-step* scheme.

The background underneath the transition peak was thus reduced by more than two orders of magnitude compared to the *one-step* scheme described earlier. As a result the effective noise temperature of this detector system, intrinsically determined by the background contributions due to the tail contaminations from the initially prepared lower state, is well below 10 mK with this scheme. Thus the present method of field ionization detection satisfies the most important requirement of low noise characteristics for a sensitive microwave single-photon detector.

In conclusion, we have established a quite stringent method to selectively ionize the low ℓ states which lie below and above the adjacent manifold by properly manipulating the ionization path through the pulsed electric field. With more sophisticated pulse profile of three steps further, which has the holding time in between the steeply rising field for ionization, the selectivity is much more enhanced due to the characteristics of the ionization mechanism in these highly excited Rydberg atoms. Two actual schemes were proposed and experimentally demonstrated to be practical and effective for this purpose. It was shown in particular that the *backward driving* scheme is more efficient for the Rydberg atoms to be utilized as the microwave single photon detector. The present method thus opens a new way to detect single microwave photons individually over the region of 10 cm wavelength with higher n Rydberg atoms[4,10].

This research was partly supported by a Grant-in-aid for Specially Promoted Research by the Ministry of Education, Science, Sports, and Culture, Japan (No. 09102010). M.T., S.Y., and T.H. thank the financial support of JSPS, Japan under the Research Fellowships for the Young Scientists.

References

- [1] *Rydberg States of Atoms and Molecules*, eds. R.F. Stebbings and F. B. Dunning (Cambridge University Press, Cambridge, 1983).
- [2] T. F. Gallagher, *Rydberg Atoms* (Cambridge University Press, Cambridge, 1994) and references cited therein.
- [3] D. Kleppner and T. W. Ducas, *Bull. Am. Phys. Soc.* 21 (1976) 600; T. W. Ducas, W. P. Spencer, A. G. Vaidyanathan, W. H. Hamilton, and D. Kleppner, *Appl. Phys. Lett.* 35 (1979) 382; H. Figger, G. Leuchs, R. Straubinger, and H. Walther, *Opt. Comm.* 33 (1980) 37; P. Goi, *et al.*, *Phys. Rev. A* 27 (1983) 2065.
- [4] S. Matsuki and K. Yamamoto, *Phys. Lett.* 263 (1991) 523; I. Ogawa, S. Matsuki and K. Yamamoto, *Phys. Rev. D* 53 (1996) R1740.
- [5] Recent review includes *Cavity Quantum Electrodynamics*, edited by P. Berman (Academic Press, Boston, 1994); A. Rauschenbeutel *et al.*, *Phys. Rev. Lett.* 83 (1999) 5166; J. M. Raimond, M. Brune, and S. Haroche, *Rev. Mod. Phys.* 73 (2001) 565.
- [6] Y. Kishimoto *et al.*, LANL.arXiv.org e-Print archive, physics/0204038 (<http://xxx.lanl.gov/>).
- [7] D. A. Harmin, *Phys. Rev. A* 44 (1991) 433.
- [8] C. Higgs, M. A. Fineman, F. B. Dunning, R. F. Stebbings, *J. Phys.* B15 (1982) L697; D. R. Mariani, W. van de Water, P. M. Koch, and T. Bergeman, *Phys. Rev. Lett.* 50 (1983) 1261; R. G. Rolfes, D. B. Smith, and K. B. MacAdam, *J. Phys.* B15 (1982) L697.
- [9] Y. Kishimoto, *Memoir of Faculty of Science, Kyoto Univ. Ser. Phys.*, 38 (2002) 163.
- [10] M. Tada, *et al.*, *Nucl. Phys.* B72 (1999) 164.